



Article

Systematic Performance Analysis of Hybrid FSO/RF System over Generalized Fading Channels with Pointing Errors

Yan Wu ^{1,†} , Mengwan Jiang ^{2,†}, Gang Li ¹ and Dejin Kong ^{1,*} 

¹ The State Key Laboratory of New Textile Materials and Advanced Processing Technologies, School of Electronic and Electrical Engineering, Wuhan Textile University, Wuhan 430200, China

² School of Artificial intelligence and Big Data, Henan University of Technology, Zhengzhou 450001, China

* Correspondence: djkou@wtu.edu.cn

† These authors contributed equally to this work.

Abstract: Hybrid free space optical (FSO)/radio frequency (RF) system has attracted extensive attention because of its advantages of both the FSO and RF links. From the viewpoint of overall system performance, this paper presents a systematic analysis method of communication performance and security performance of the hybrid FSO/RF system with the Málaga turbulence channel and the $\alpha - \mu$ fading channel. The hybrid FSO/RF system adopts the diversity method of maximum ratio combining (MRC) to receive signals. The new expressions of communication performance parameters (i.e., the bit error rate, the outage probability, the ergodic channel capacity) of the only FSO system and the hybrid system are obtained. Then, the new expressions of the security performance parameters (i.e., the security outage probability and the strictly positive secrecy capacity) of the hybrid system with the FSO or RF links eavesdropping are derived, respectively. Our derived analytical expressions present an efficient tool to investigate the impact of system parameters on the overall performance of the hybrid system, namely modulation scheme, turbulence intensity, pointing errors, target rate, and eavesdropper output signal-to-noise ratio. The simulation results show that compared with the only FSO system, the hybrid system can significantly improve the communication performance of the system; the communication performance of the hybrid system using coherent binary phase shift keying (CBPSK) modulation is obviously better than the other two modulation technologies; with the deterioration of atmospheric environment (increasing turbulence intensity and pointing errors), the communication performance and security performance of the hybrid system will decline; both RF link eavesdropping and FSO link eavesdropping have a greater impact on the security performance of the hybrid systems; whether it is FSO link eavesdropping or RF link eavesdropping, the reduction of target rate and output signal-to-noise ratio of the eavesdropper can improve the security performance of the hybrid system.

Keywords: hybrid FSO/RF system; communication performance; security performance; atmospheric turbulence; pointing errors



Citation: Wu, Y.; Jiang M.; Li, G.; Kong D. Systematic Performance Analysis of Hybrid FSO/RF System over Generalized Fading Channels with Pointing Errors. *Photonics* **2022**, *9*, 873. <https://doi.org/10.3390/photonics9110873>

Received: 13 October 2022

Accepted: 10 November 2022

Published: 18 November 2022

Publisher's Note: MDPI stays neutral with regard to jurisdictional claims in published maps and institutional affiliations.



Copyright: © 2022 by the authors. Licensee MDPI, Basel, Switzerland. This article is an open access article distributed under the terms and conditions of the Creative Commons Attribution (CC BY) license (<https://creativecommons.org/licenses/by/4.0/>).

1. Introduction

1.1. Background

A free space optical (FSO) communication system has many advantages such as license-free spectrum, low cost, easy installation, and high transmission bandwidth, and is considered an alternative to next-generation mobile communication [1,2]. However, the free space optical communication system is seriously affected by the channel environment (atmospheric turbulence and pointing errors) [3]. Atmospheric turbulence is caused by the random change of the atmospheric temperature field due to the influence of surface radiation, solar radiation, atmospheric flow, and other factors. Atmospheric turbulence can lead to beam broadening and beam wandering, which can degrade the communication performance of the FSO system. The pointing error is caused by the sway of the building

or the jitter of the communication device, which also can degrade the communication performance of the FSO system, even the interruption of communication.

Therefore, previous works have proposed various mitigation technologies to improve the performance of the FSO communication system. Adaptive optics technology can overcome the beam wander caused by atmospheric turbulence [4]. To solve the misalignment caused by building vibration, the ATP (acquisition, tracking, and pointing) technology is proposed [5]. In addition, the performance of the FSO communication system can be improved by using a high-performance beam [6], spatial diversity [7], hybrid FSO/radio frequency (RF) communication scheme [8], and other technologies [9–14].

Compared with the FSO link, atmospheric environment have little impact on the RF link, such as fog, turbulence, and so on. The communication scheme of the hybrid FSO and RF parallel transmission can combine the advantages of the FSO link and RF link to improve the performance of the communication system. Shakir et al. [15] proposed a hybrid parallel communication system based on an FSO link with Gamma-Gamma distribution and an RF link with Rayleigh distribution and derived new closed-form expressions for its average bit error rate (BER) and outage probability (OP). Tahami et al. [16] proposed a hybrid serial transmission system of the RF link with Rayleigh distribution and the FSO link with the Gamma-Gamma distribution, the system adopted an amplify and forward (AF) relay with variable gain as a relay device and deduced new closed-form expressions of the BER and OP. Altubaishi et al. [17] gave an approximate expression of the ergodic channel capacity (ECC) of the FSO multi-hop hybrid system combined with an RF backup link and AF relay and analyzed the influence of weather conditions on the hybrid system.

In addition, the hybrid FSO/RF communication system has great potential to improve the performance of the communication system. For example, the hybrid FSO/RF parallel multi-hop system can not only improve the transmission distance but also improve the system performance [18]. The performance of hybrid FSO/RF systems can be further improved by using wavelength division multiplexing (WDM) and spatial diversity in FSO links, or by using multiple input multiple output (MIMO) technology in RF links [19–21]. Therefore, a comprehensive study of the performance of hybrid FSO/RF communication systems is of great significance to engineering practice and theoretical research.

1.2. Related Works

Hybrid FSO/RF parallel systems can be divided into two categories: mode switching systems and parallel transmission systems. In a hybrid FSO/RF system with mode switching, the RF link acts as a backup connection. The system switches to the RF link only when the instantaneous SNR of the primary FSO link is lower than a predefined threshold [22–24]. However, this mode switching system largely depends on the availability of feedback information or channel state information (CSI) on the system transceiver, which increases the system hardware complexity. Vishwakarma et al. [25] derived the closed-form expressions of the OP, symbol error rate (SER), and ECC of the hybrid FSO/RF system with hard switching mode.

On the other hand, in a hybrid FSO/RF system with parallel transmission, the same data will be transmitted on two links at the same time. In addition, the received signals will be processed by diversity combining at the system receiving end before signal demodulation, such as maximum ratio combining (MRC), equivalent gain combining (EGC), selective combining (SC), and adaptive combining (AC) [26–28]. Therefore, this scheme does not require feedback information or CSI to realize the switching operation between two links. Compared with the mode switching system, the parallel transmission system has the advantages of simplicity and economy. Liang et al. [29] derived the closed-form expressions of the OP and BER of the hybrid FSO/RF system with SC and pointing errors (PE). Chatzidiamantis et al. [30] approximately analyzed the BER performance of hybrid FSO/RF systems with MRC and SC schemes.

In the recent years, as an effective scheme against eavesdropping in the wireless communication system, physical layer security has been introduced into the RF or FSO

communication links. This strategy makes use of the inherent random characteristics of the wireless channel to improve system security [31]. Lei et al. [32] studied the security performance of the FSO links subject to Gamma-Gamma distribution and deduced the closed expressions of the lower bounds of strict positive security capacity (SPSC) and security outage probability (SOP).

At present, research on physical layer security mainly focuses on hybrid FSO/RF systems in the open literature, while research on physical layer security of hybrid FSO/RF communication systems is rare. Juel et al. [33] deduced the new closed-form expressions of average security capacity (ASC), SOP, and SPSC of mixed dual-hop RF/FSO system when the relay scheme is based on an AF relay and RF link eavesdropping. Yang et al. [34] studied the average security rate (ASR) and SOP performance of the mixed FSO/RF dual-hop communication system during RF link eavesdropping under fixed gain and variable gain relay schemes. Mehta et al. [35] derived and analyzed the expressions of the OP, outage capacity (OC) and SOP of the hybrid FSO/RF system with modified switching. Shakir et al. [36] derived and analyzed the expressions of the SOP, SPSC, and ASC of the hybrid FSO/RF system with selective combining under RF colluding and non-colluding eavesdropping scenarios.

However, current research on the physical layer security of the hybrid FSO/RF system mainly considers RF eavesdropping, while research on the physical layer security of the hybrid system with FSO link eavesdropping is rare. Tokgoz et al. [37] derived and analyzed the expressions of the SPSC of the hybrid FSO/RF system with selective combining under three different types of eavesdroppers. However, the impact of the FSO link pointing error on security performance is not taken into account.

1.3. Motivation and Contributions

To the best of our knowledge, the security performance analysis of the hybrid FSO/RF system with MRC scheme has not yet been fully investigated when FSO link eavesdropping is considered, and few studies have been found on the ECC of hybrid FSO/RF parallel transmission systems. Because the hybrid FSO/RF parallel transmission system uses two different communication links for information transmission at the same time, the hybrid system is more vulnerable to malicious eavesdropping than the traditional only RF communication or only FSO communication. At present, research on the communication performance and security performance of the hybrid FSO/RF system is relatively independent, and no analysis has been made on the impact of the ECC on the security performance of the system. A comprehensive and systematic analysis of the communication performance and security performance of the hybrid FSO/RF system is of great significance to theoretical analysis and engineering practice.

In this work, from the perspective of the overall performance analysis of the hybrid FSO/RF system, we take an interest in the communication performance and security performance analysis of the hybrid system with atmospheric turbulence and pointing errors. First of all, the probability density function (PDF) and cumulative distribution function (CDF) of the signal-to-noise ratio (SNR) at the receiver of the FSO link with the Málaga distribution, and the PDF and CDF of the SNR at the receiver of the RF link subject to the $\alpha - \mu$ distribution are given. Then, the PDF and CDF of the SNR at the receiver of the hybrid FSO/RF parallel system based on the MRC scheme are derived. Next, the new expressions of the communication performance parameters such as BER, OP, and ECC of the hybrid system and the only FSO system are derived. Moreover, the new expressions of the security performance parameters such as the SOP and the SPSC of the hybrid system in the case of FSO link eavesdropping and RF link eavesdropping are derived, respectively. Finally, numerical results, which demonstrate the communication performance and security performance of the FSO/RF system with atmospheric turbulence and pointing errors, are presented. Table 1 compares the existing work of the hybrid FSO/RF system with the main research contents of this paper in detail.

Table 1. Comparison of research contents between the relevant literature and this paper on the hybrid FSO/RF parallel transmission system.

Ref.	Switch/Combination	Modulation	Detection	FSO Channel	RF Channel	PE	Eavesdropper	Metrics
[22]	hard switching	PSK	DD	Log-normal	Nakagami-m	✗	✗	BER, OP, ECC
[23]	hard switching	OOK, 16-QAM	DD	Gamma-Gamma	Rician	✓	✗	BER, OP
[25]	hard switching	M-PSK	HD, DD	Málaga	$\alpha - \eta - \kappa - \mu$	✓	✗	SER, OP, ECC
[15]	SC	M-PSK	DD	Gamma-Gamma	Rayleigh	✗	✗	BER, OP
[29]	SC	M-PSK	DD	Gamma-Gamma	Nakagami-m	✓	✗	BER, OP
[30]	MRC, SC	PSK	DD	Gamma-Gamma	Rician	✗	✗	BER
[38]	MRC, SC	OOK, M-PSK, M-QAM	HD, DD	Gamma-Gamma	$\kappa - \mu$	✗	✗	BER, OP
[26]	SC	PSK, FSK	HD, DD	Gamma-Gamma	Nakagami-m	✓	✗	BER, OP, ECC
[28]	AC	✗	HD, DD	Gamma-Gamma	$\kappa - \mu$	✓	✗	ECC
[27]	SC	PSK, FSK	DD	Málaga	$\eta - \mu$	✓	RF	BER, OP, SOP
[35]	Modified switching	BPSK	DD	Gamma-Gamma	Exponential	✓	RF	OP, OC, SOP
[36]	SC	✗	HD, DD	Málaga	Nakagami-m	✗	RF	SOP, SPSC, ASC
[37]	MRC	✗	DD	Gamma-Gamma	Nakagami-m	✗	FSO, RF, hybrid	SPSC
This	MRC	OOK, M-PSK, M-QAM	HD, DD	Málaga	$\alpha - \mu$	✓	FSO, RF	BER, OP, ECC, SOP, SPSC

Our main contributions in this work are pointed out as follows:

- We first obtain the PDF and CDF of the SNR at the receiver of the hybrid FSO/RF parallel system with the MRC scheme and pointing errors.
- Through the analysis of communication performance, the new expressions of communication performance parameters such as the BER, OP, and ECC of the hybrid system and the only FSO system are derived. These expressions are novel compared to the existing works as the hybrid FSO/RF model with Málaga turbulence and $\alpha - \mu$ fading is not reported in the existing hybrid FSO/RF literature, and the ECC of the hybrid system is also rarely reported.
- Through the analysis of the security performance, the new expressions of the security performance parameters of the hybrid system, such as the SOP and SPSC, are derived, respectively, in the case of the FSO link eavesdropping or the RF link eavesdropping. These expressions are novel compared to the existing works as the effect of FSO link eavesdropping is not reported in the existing hybrid FSO/RF with MRC technique literature.
- Through the method of system simulation, we not only compare and analyze the communication performance and security performance of the hybrid system by different turbulence intensity and pointing errors, but also compare and analyze the SOP and SPSC of the hybrid system with FSO link eavesdropping and RF link eavesdropping. In addition, the security performance of the system is explained by using the analysis conclusion of the ECC, which has not been seen in previous work. Compared with the existing work, these simulation and analysis works are innovative as such a systematic and comprehensive performance analysis has not been reported in the existing hybrid FSO/RF literature.

The paper is structured as follows. In Section 2, we present the system model of the hybrid system with atmospheric turbulence and pointing errors. In Section 3, we analyze the communication performances of the hybrid system, and the only FSO link or the only RF link. In Section 4, we analyze the security performances of the hybrid system with FSO link eavesdropping and RF link eavesdropping. In Section 5, we show the simulation results around the performances of the hybrid system. In Section 6, we finally summarize the whole paper.

2. System and Channel Model

At the transmitter of the hybrid FSO/RF parallel system, the signal is separated into two signals after binary modulation (on-off keying, OOK; multilevel phase shift keying, M-PSK; multilevel quadrature amplitude modulation, M-QAM) and sent to FSO and RF subsystems, respectively. In the FSO subsystem, the transmitter sends the modulated signal light to the FSO channel by using intensity modulation, and the receiver can demodulate the received optical signal in two ways: Direct detection and heterodyne detection. In the RF

subsystem, the transmitter upconverts the modulated signal to the millimeter wave (MMW) RF frequency of 60 GHz, and then sends the MMW signal to the RF channel. In addition, the receiver will down-convert and demodulate the MMW signal and retrieve it to the original signal. Finally, the received signals of the FSO and RF links are combined in a certain proportion at the receiving end of the hybrid system, that is the MRC scheme. Because the hybrid FSO/RF parallel transmission system will transmit the same information on two different physical links at the same time, it may encounter two different eavesdropping modes: the FSO link eavesdropping and the RF link eavesdropping, as shown in Figure 1. At the transmitter of the hybrid FSO/RF parallel system, the signal is separated into two signals after binary modulation and subcarrier pre-modulation and modulated to optical and RF carriers, respectively. These carriers are then sent to FSO and RF communication links through the transmitter for transmission, and the received signals of the FSO and RF links are combined in a certain proportion at the receiving end of the hybrid system. For the communication system in which two different links transmit the same information at the same time, there may be two eavesdropping modes: the FSO link eavesdropping and the RF link eavesdropping.

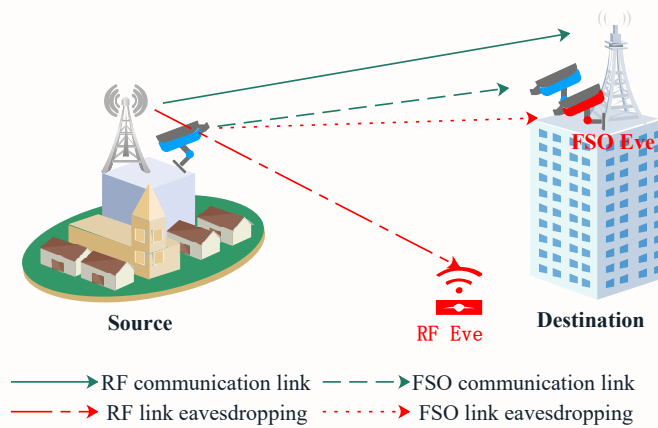


Figure 1. Hybrid FSO/RF system model with RF or FSO link eavesdropping.

2.1. FSO Sublink

Considering the Málaga atmospheric turbulence model and pointing errors, the PDF of instantaneous SNR γ^{FSO} at the output of the FSO sublink is [39]:

$$f_{\gamma^{FSO}}(\gamma^{FSO}) = \frac{\xi^2 A}{2^r \gamma^{FSO}} \sum_{k=1}^{\beta} b_k G_{1,3}^{3,0} \left(B \left(\frac{\gamma^{FSO}}{\mu^{FSO,r}} \right)^{\frac{1}{r}} \middle| \begin{matrix} 1 + \xi^2 \\ \xi^2, \alpha, k \end{matrix} \right) \tag{1}$$

where $G_{1,3}^{3,0}(\cdot)$ is the Meijer-G function, and ξ is the ratio of the equivalent beam radius of the receiver plane to the jitter standard deviation of the receiver plane, which represents the degree of deviation of the beam from the boresight. For example, the greater the value of ξ , the smaller the deviation of the beam from the boresight. $A = \frac{2\alpha^{\alpha/2}}{g^{1+\alpha/2}\Gamma(\alpha)} \left(\frac{g\beta}{g\beta+\Omega'} \right)^{\beta+\frac{\alpha}{2}}$, $B = \frac{\xi^2 \alpha \beta (g\beta+\Omega')}{(\xi^2+1)(g\beta+\Omega')}$, $a_k = \binom{\beta-1}{k-1} \frac{(g\beta+\Omega')^{1-\frac{k}{2}}}{(k-1)!} \left(\frac{\Omega'}{g} \right)^{k-1} \left(\frac{\alpha}{\beta} \right)^{k/2}$, $b_k = a_k [\alpha\beta / (g\beta + \Omega')]^{-(\alpha+k)/2}$, k is a summation variable and $\Gamma(\cdot)$ is the Gamma function. α is a positive parameter, which is related to the effective number of large-scale vortices in the scattering process, and β is the value of the fading parameter. $g = 2b_0(1 - \rho)$ represents the average power of the independent scattering component received by the off-axis eddies path, $2b_0$ is the average power of the total scattering component, $\rho \in [0, 1]$ represents the scattering power value

coupled with the line of sight component, Ω' is the average power of mutual coupling components. $\mu^{FSO,r}$ represents the average SNR of the FSO sub-link, r is the parameter that defines the detection technology, that is, $r = 1$ represents heterodyne detection (HD) and $r = 2$ represents direct detection (DD). When $r = 1$, $\mu^{FSO,1} = \mu_{HD} = \bar{\gamma}^{FSO}$. When $r = 2$, $\mu^{FSO,2} = \mu_{DD} = \frac{\alpha \xi^2 (\xi^2 + 1)^{-2} (\xi^2 + 2)(g + \Omega')}{(\alpha + 1) [2g(g + 2\Omega') + \Omega'^2 (1 + \frac{1}{\beta})]} \mu^{FSO,1}$.

By applying the integral identity $F_{\gamma^{FSO}}(\gamma^{FSO}) = \int_0^{\gamma^{FSO}} f_{\gamma^{FSO}}(t) dt$ to (1), the CDF of γ^{FSO} can be obtained as:

$$F_{\gamma^{FSO}}(\gamma^{FSO}) = D \sum_{k=1}^{\beta} c_k G_{r+1,3r+1}^{3r,1} \left(E \frac{\gamma^{FSO}}{\mu^{FSO,r}} \middle| \begin{matrix} 1, \kappa_1 \\ \kappa_2, 0 \end{matrix} \right) \tag{2}$$

where $D = \xi^2 A / [2^r (2\pi)^{r-1}]$, $c_k = b_k r^{\alpha+k-1}$, $E = B^r / r^{2r}$, $\kappa_1 = (\xi^2 + 1)/r, \dots, (\xi^2 + r)/r$ (includes r items), $\kappa_2 = \xi^2/r, \dots, (\xi^2 + r - 1)/r, \alpha/r, \dots, (\alpha + r - 1)/r, k/r, \dots, (k + r - 1)/r$ (includes $3r$ items) to simplify the expression. It is worth noting that the Málaga distribution has unified most of the existing uniform and isotropic turbulence mathematical models in Table 1 of [40], such as the Gamma-Gamma distribution, Lognormal distribution, K distribution, and so on.

2.2. RF Sublink

Assuming that the channel of the RF link adopts the $\alpha - \mu$ distribution model, the PDF of instantaneous SNR γ^{RF} at the output of the RF sublink can be written as follows [33]:

$$f_{\gamma^{RF}}(\gamma^{RF}) = A_m e^{-B_m (\gamma^{RF})^{C_m}} (\gamma^{RF})^{C_m \mu_m - 1}, \tag{3}$$

where $A_m = \frac{C_m B_m^{\mu_m}}{\Gamma(\mu_m)}$, $B_m = \mu_m (\bar{\gamma}^{RF})^{-C_m}$, $C_m = \frac{\alpha_m}{2}$, and $\bar{\gamma}^{RF}$ is the output average SNR of the RF sublink. $\alpha_m > 0$ and $\mu_m > 0$ represent the nonlinearity parameter of the propagation environment and the number of multipath clusters, respectively. The $\alpha - \mu$ distribution is the unified model which includes the small-scale fading channel and the large-scale fading channel. Some classical RF channel models can be obtained by setting different values of α_m and μ_m [33,41].

The CDF of γ^{RF} can be obtained by the integral [33]:

$$F_{\gamma^{RF}}(\gamma^{RF}) = 1 - D_m e^{-B_m \gamma^{C_m}} \gamma^{j C_m}, \tag{4}$$

where $D_m = \sum_{j=0}^{\mu_m-1} \frac{1}{j!} B_m^j$.

2.3. Hybrid FSO/RF System Based on MRC Scheme

For the MRC scheme, it is assumed that the output SNR of the hybrid FSO/RF system is $\gamma^{MRC} = \gamma^{FSO} + \gamma^{RF}$. Since the FSO sub-link and the RF sub-link are independent, the PDF of γ^{MRC} can be written as:

$$f_{\gamma^{MRC}}(\gamma) = \int_0^{\gamma} f_{\gamma^{FSO}}(t) f_{\gamma^{RF}}(\gamma - t) dt \tag{5}$$

By substituting (1) and (3) in (5), it can be rewritten as

$$f_{\gamma^{MRC}}(\gamma) = A_1 \sum_{k=1}^{\beta} c_k \sum_{i=0}^{\infty} C_1 \gamma^{D_1-1} G_{r+1,3r+1}^{3r,1} \left(E_1 \gamma \middle| \begin{matrix} 1, \kappa_1 \\ \kappa_2, 1 - D_1 \end{matrix} \right) \tag{6}$$

where $A_1 = \frac{\xi^2 A_m A}{2^{2r-1} \pi^{r-1}}$, $C_1 = \frac{(-B_m)^i \Gamma(D_1)}{i!}$, $D_1 = C_m (\mu_m + i)$, $E_1 = \frac{E}{\mu^{FSO,r}}$.

The CDF of γ^{MRC} obtained by integrating Equation (6) can be expressed as

$$F_{\gamma^{MRC}}(\gamma) = A_1 \sum_{k=1}^{\beta} c_k \sum_{i=0}^{\infty} C_1 \gamma^{D_1} G_{r+2,3r+2}^{3r,2} \left(E_1 \gamma \left| \begin{matrix} 1 - D_1, 1, \kappa_1 \\ \kappa_2, 1 - D_1, -D_1 \end{matrix} \right. \right) \quad (7)$$

3. Communication Performance Analysis of Hybrid FSO/RF System

3.1. Average Bit Error Rate

For the hybrid FSO/RF system, a binary modulation scheme is used for data transmission in the FSO or RF link. According to [42], the average BER of the hybrid system which is based on the binary modulation techniques can be expressed as:

$$P_b = \frac{\delta}{2\Gamma(p)} \sum_{t=1}^n q_t^p \int_0^{\infty} \gamma^{p-1} e^{-q_t \gamma} F_{\gamma^{MRC}}(\gamma) d\gamma \quad (8)$$

where n , δ , p , and q_t represent various modulation schemes and detection types according to Table 2 [38,42,43]. It is worth noting that some conditions have not been taken into account in the analysis of the BER, such as the thermal noise variance, shot noise, amplified spontaneous emission (ASE), weather, and climate conditions.

Table 2. Parameters for different modulation schemes.

Binary Modulation Scheme	Detection Type	δ	p	q_t	n
OOK	DD	1	1/2	1/2	1
M-PSK	HD	$\frac{2}{\max(\log_2 M, 2)}$	1/2	$\sin^2\left(\frac{(2t-1)\pi}{M}\right)$	$\max\left(\frac{M}{4}, 1\right)$
M-QAM	HD	$\frac{4}{\log_2 M} \left(1 - \frac{1}{\sqrt{M}}\right)$	1/2	$\frac{3(2t-1)^2}{2(M-1)}$	$\frac{\sqrt{M}}{2}$

Substituting (7) in (8) and applying $e^{-x} = G_{0,1}^{1,0} \left(x \left| \begin{matrix} - \\ 0 \end{matrix} \right. \right)$ and Equation (07.34.21.0088.01) in [44], the average BER of the hybrid system can be obtained:

$$P_b^{hy} = \frac{\delta A_1}{2\Gamma(p)} \sum_{t=1}^n \sum_{k=1}^{\beta} \sum_{i=0}^{\infty} c_k C_1 q_t^{-D_1} G_{r+3,3r+2}^{3r,3} \left(\frac{E_1}{q_t} \left| \begin{matrix} 1 - D_1 - p, 1 - D_1, 1, \kappa_1 \\ \kappa_2, 1 - D_1, -D_1 \end{matrix} \right. \right), \quad (9)$$

By substituting Equation (2) into Equation (8), the average BER of the only FSO link can be obtained:

$$P_b^{FSO} = \frac{D\delta}{2\Gamma(p)} \sum_{t=1}^n \sum_{k=1}^{\beta} c_k G_{r+2,3r+1}^{3r,2} \left(\frac{E}{\mu^{FSO,r} q_t} \left| \begin{matrix} 1 - p, 1, \kappa_1 \\ \kappa_2, 0 \end{matrix} \right. \right) \quad (10)$$

3.2. Outage Probability

Outage probability is the probability when the end-to-end output SNR of the communication system is lower than a specific threshold γ_{th} [45]. Therefore, the OP of the hybrid system can be expressed as:

$$P_{out} = \Pr(\gamma^{MRC} < \gamma_{th}) = \int_0^{\gamma_{th}} f_{\gamma^{MRC}}(\gamma) d\gamma = F_{\gamma^{MRC}}(\gamma_{th}). \quad (11)$$

By substituting Equation (7) into Equation (11), the OP of the hybrid system can be rewritten as:

$$P_{out}^{hy} = A_1 \sum_{k=1}^{\beta} c_k \sum_{i=0}^{\infty} C_1 \gamma_{th}^{D_1} G_{r+2,3r+2}^{3r,2} \left(E_1 \gamma_{th} \left| \begin{matrix} 1 - D_1, 1, \kappa_1 \\ \kappa_2, 1 - D_1, -D_1 \end{matrix} \right. \right) \quad (12)$$

According to the definition of outage probability, the OP of the only FSO system can be directly given by substituting Equation (2) into Equation (11).

3.3. Ergodic Channel Capacity

In time-varying channels, the ergodic channel capacity is the weighted average of the capacity of the system in each channel state [46]. The normalized ECC of the hybrid FSO/RF system can be obtained by the following equation [47]:

$$\langle C \rangle = \int_0^\infty \log_2(1 + \gamma) f_{\gamma^{MRC}}(\gamma) d\gamma. \tag{13}$$

Using the relationship between functions: $\log_2(1 + x) = \frac{1}{\ln 2} G_{2,2}^{1,2} \left(x \middle| \begin{matrix} 1, 1 \\ 1, 0 \end{matrix} \right)$ and $e^{-x} = G_{0,1}^{1,0} \left(x \middle| \begin{matrix} - \\ 0 \end{matrix} \right)$ [48,49] and Equation (07.34.21.0011.01) in [44], by substituting Equation (6) into Equation (13), the ECC of the hybrid system can be obtained as

$$\langle C^{hy} \rangle = \frac{A_1}{\ln 2} \sum_{k=1}^{\beta} c_k \sum_{i=0}^{\infty} C_1 G_{r+3,3r+3}^{3r+2,2} \left(E_1 \middle| \begin{matrix} 1 - D_1, 1 - D_1, \kappa_1 \\ \kappa_2, -D_1, -D_1, 1 - D_1 \end{matrix} \right) \tag{14}$$

According to Equation (07.34.21.0012.01) in [44], the ECC of the only FSO system can be obtained by substituting Equation (1) into Equation (13):

$$\langle C^{FSO} \rangle = \frac{\xi^2 A}{2^r \ln 2} \sum_{k=1}^{\beta} b_k H_{3,5}^{5,1} \left(\frac{B}{(\mu^{FSO,r})^{1/r}} \middle| \begin{matrix} \kappa_3 \\ \kappa_4 \end{matrix} \right) \tag{15}$$

where $\kappa_3 = (0, 1/r), (1, 1/r), (1 + \xi^2, 1)$, $\kappa_4 = (\xi^2, 1), (\alpha, 1), (k, 1), (0, 1/r), (0, 1/r)$, and $H_{\cdot}^{\cdot}(\cdot)$ is the Fox-H function [50].

According to Equation (07.34.21.0012.01) in [44], the ECC of the only RF system can be obtained by substituting Equation (3) into Equation (13):

$$\langle C^{RF} \rangle = \frac{A_m}{\ln 2} H_{2,3}^{3,1} \left(B_m \middle| \begin{matrix} \kappa_5 \\ \kappa_6 \end{matrix} \right) \tag{16}$$

where $\kappa_5 = (-C_m \mu_{mv}, C_m), (1 - C_m \mu_{mv}, C_m)$ and $\kappa_6 = (0, 1), (-C_m \mu_{mv}, C_m), (-C_m \mu_{mv}, C_m)$.

4. Security Performance Analysis of Hybrid FSO/RF System

4.1. Security Outage Probability

In the physical layer security theory, the security outage probability is the probability that the instantaneous security capacity C_s is lower than the target rate R_s ($R_s > 0$). The SOP is usually considered an important parameter to evaluate the security performance of the wireless communication system. According to [32], the definition formula of SOP can be written as:

$$\begin{aligned} SOP &= Pr \left\{ C_s(\gamma^{MRC}, \gamma^E) \leq R_s \right\} \\ &\triangleq Pr \left\{ \gamma^{MRC} \leq \Theta \gamma^E + \Theta - 1 \right\} \\ &\triangleq \int_0^\infty F_{\gamma^{MRC}}(\Theta \gamma^E + \Theta - 1) f_{\gamma^E}(\gamma^E) d\gamma^E, \end{aligned} \tag{17}$$

where $\Theta = \exp(R_s) \geq 1$ and $f_{\gamma^E}(\gamma^E)$ is the PDF of the eavesdropping channel. It should be noted that the eavesdropping channel can be either the RF link or FSO link, that is, $\gamma^E = \gamma^{RF}$ or $\gamma^E = \gamma^{FSO}$.

According to the method provided in [32], assuming $\gamma^E \rightarrow \infty$, the lower bound of the SOP of the hybrid system can be given:

$$SOP_L = \int_0^\infty F_{\gamma^{MRC}}(\Theta\gamma) f_{\gamma^E}(\gamma) d\gamma. \tag{18}$$

(1) RF link eavesdropping

By substituting Equations (3) and (7) into Equation (18), the SOP of the hybrid system with the RF link eavesdropping can be given by

$$SOP_L^{RF}(R_s) = A_1 A_m^E \sum_{k=1}^{\beta} c_k \sum_{i=0}^{\infty} C_1 \Theta^{D_1} \cdot \int_0^\infty (\gamma)^{C_m^E \mu_m^E + D_1 - 1} e^{-B_m^E(\gamma)^{C_m^E}} \cdot G_{r+2, 3r+2}^{3r, 2} \left(E_1 \Theta \gamma \left| \begin{matrix} 1 - D_1, 1, \kappa_1 \\ \kappa_2, 1 - D_1, -D_1 \end{matrix} \right. \right) d\gamma \tag{19}$$

According to Equation (07.34.21.0012.01) in [44] and Equation (8.4.3.1) in [48], Equation (19) can be simplified as:

$$SOP_L^{RF}(R_s) = A_1 A_m^E \sum_{k=1}^{\beta} c_k \sum_{i=0}^{\infty} C_1 \Theta^{D_1} (E_1 \Theta)^{-C_m^E \mu_m^E - D_1} H_{3r+2, r+3}^{3, 3r} \left(\frac{B_m^E}{(E_1 \Theta)^{C_m^E}} \left| \begin{matrix} \kappa_7 \\ \kappa_8 \end{matrix} \right. \right) \tag{20}$$

where $\kappa_7 = (1 - C_m^E \mu_m^E - D_1 - \kappa_2, C_m^E), (-C_m^E \mu_m^E, C_m^E), (1 - C_m^E \mu_m^E, C_m^E)$ and $\kappa_8 = (0, 1), (-C_m^E \mu_m^E, C_m^E), (-C_m^E \mu_m^E - D_1, C_m^E), (1 - C_m^E \mu_m^E - D_1 - \kappa_1, C_m^E)$.

(2) FSO link eavesdropping

Due to the close location of the FSO eavesdropping device and the FSO communication receiver, it can be considered that the FSO eavesdropping link and the FSO communication link have experienced the same turbulent environment, but the beam jitter on the plane of the two receivers is different. We modify all parameters (i.e., $g \rightarrow g^E, F \rightarrow F^E, B \rightarrow B^E$, and $c_k \rightarrow c_k^E$) in Equation (1), and then bring them into Equation (18) with Equation (7). The SOP of the hybrid system with the FSO link eavesdropping can be obtained after a series of algebraic operations:

$$SOP_L^{FSO}(R_s) = \frac{(\xi^E)^2 A^E A_1}{2^{r^E}} \sum_{k=1}^{\beta} c_k \sum_{i=0}^{\infty} C_1 \Theta^{D_1} \sum_{k^E=1}^{\beta^E} b_{k^E}^E (E_1 \Theta)^{-D_1} H_{3r+3, r+5}^{5, 3r} \left(E_2 \left| \begin{matrix} \kappa_9 \\ \kappa_{10} \end{matrix} \right. \right) \tag{21}$$

where $E_2 = B^E (E_1 \Theta \mu^{E, r^E})^{-\frac{1}{r^E}}, \kappa_9 = (1 - D_1 - \kappa_2, \frac{1}{r^E}), (0, \frac{1}{r^E}), (1, \frac{1}{r^E}), (1 + (\xi^E)^2, 1)$, and $\kappa_{10} = ((\xi^E)^2, 1), (\alpha^E, 1), (k^E, 1), (0, \frac{1}{r^E}), (-D_1, \frac{1}{r^E}), (1 - D_1 - \kappa_1, \frac{1}{r^E})$.

4.2. Strict Positive Security Capacity

Strict forward security capacity is defined as the probability that the instantaneous security capacity is greater than 0, which indicates the probability that the system can provide secure communication [33]. The SPSC of the hybrid system can be expressed as:

$$SPSC = P_r \{ C_s(\gamma^{MRC}, \gamma^E) > 0 \} = 1 - SOP_L|_{R_s=0}. \tag{22}$$

Substituting Equations (20) and (21) into Equation (22), the SPSC of the hybrid system with the RF link eavesdropping and the FSO link eavesdropping can be obtained, respectively.

5. Numerical Results

In this section, numerical results will be provided to analyze the communication performance and security performance of the hybrid RF/FSO system. The main simulation parameters of the hybrid FSO/RF with eavesdropper are shown in Table 3 [39,51]. Numerical results are validated by Monte Carlo simulations performed using the software package Matlab 2019(b).

Table 3. Simulation parameters of the hybrid FSO/RF with eavesdropper.

Information Transmission Link	Channel Model and Parameters
FSO communication link	Málaga turbulence, (α, β)
RF communication link	$\alpha - \mu$ fading, (α_m, μ_m)
FSO eavesdropping link	Málaga turbulence, (α^E, β^E)
RF eavesdropping link	$\alpha - \mu$ fading, (α_m^E, μ_m^E)
FSO Link	Parameter Value
Wavelength	785 nm
Link range	1 km
Laser type	Fabry–Pérot laser diodes
Beam type	Gaussian beam
Detector type	Avalanched photodiode
Weak turbulence	$(\alpha, \beta) = (\alpha^E, \beta^E) = (8, 4)$
Moderate turbulence	$(\alpha, \beta) = (\alpha^E, \beta^E) = (4.2, 3)$
Strong turbulence	$(\alpha, \beta) = (\alpha^E, \beta^E) = (2.296, 2)$
RF Link	Parameter Value
Carrier frequency	60 GHz
$\alpha - \mu$ fading	$(\alpha_m, \mu_m) = (\alpha_m^E, \mu_m^E) = (3,1)$ or $(2,1)$ or $(1,1)$
Parameters of Pointing Errors	Symbol
FSO communication link	$\zeta = 1$ or 2 or 4
FSO eavesdropping link	$\zeta^E = 1$ or 2

Without loss of generality, it is assumed that the average SNR of FSO and RF link output is equal from Figures 2–4, that is, $\bar{\gamma}^{FSO} = \bar{\gamma}^{RF}$. Figure 2 shows the relationship between the average BER and the average SNR when the hybrid FSO/RF parallel transmission system and the only FSO system adopt three sub-carrier modulation modes (CBPSK, QPSK, 4QAM) and the HD technique, respectively. The simulation conditions in Figure 2 are that the FSO link is in strong turbulence, fading parameters are $\alpha_m = 1, \mu_m = 3$, and the pointing error parameter is $\zeta = 1$. As can be seen from Figure 2, compared with the only FSO link, the hybrid system can significantly improve BER performance. From Figure 2, whether in the only FSO system or the hybrid FSO/RF system, it is evident that the system using the CBPSK modulation has the best BER performance, QPSK is the second, and 4QAM is the worst. This is because the higher the modulation order, the greater the error probability of decoding, so the BER of a high-order modulation system is higher than that of a low-order modulation system.

When the hybrid system adopts the CBPSK modulation and the fading parameters are $\alpha_m = 2, \mu_m = 1$, Figure 3 shows the relationship between the average BER and average SNR of the hybrid system under different pointing error parameters ζ and different atmospheric turbulence intensity. Figure 3 shows that when the FSO link is in weak turbulence, the greater the pointing error parameter ζ value, the more obvious the impact on the BER performance, and vice versa. Assuming that the average SNR of the system is 20 dB and the FSO link is in weak turbulence, the system BER is 2.043×10^{-5} and 1.12×10^{-6} when the pointing error parameter ζ is 1 and 2, respectively. When the FSO link environment is moderate turbulence and strong turbulence, the change of pointing error parameter ζ has an obvious effect on the BER of the hybrid system. For example, assuming that the BER of the system is 20 dB and moderate turbulence, the system BER is 2.578×10^{-5} and

42.88×10^{-6} when the pointing error parameter ζ is 1 and 2, respectively. Assuming that the BER of the system is 20 dB and strong turbulence, the BER of the system is 4.187×10^{-5} and 1.073×10^{-5} when ζ is 1 and 2, respectively.

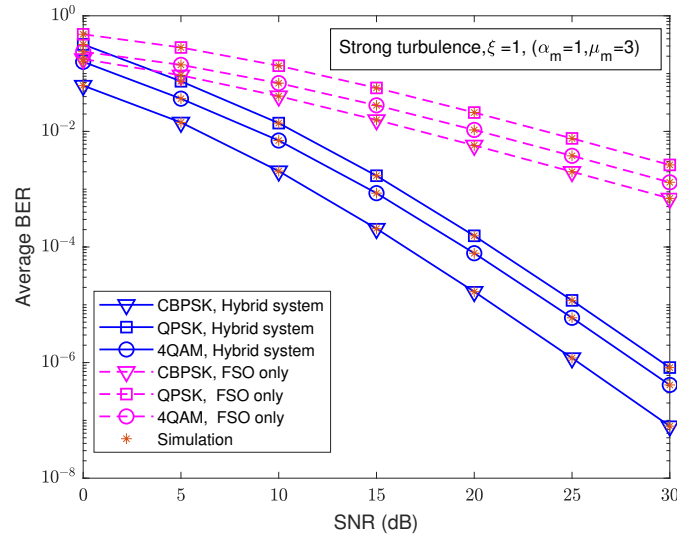


Figure 2. The relationship between BER and SNR of the hybrid system and single FSO system under different modulation modes.

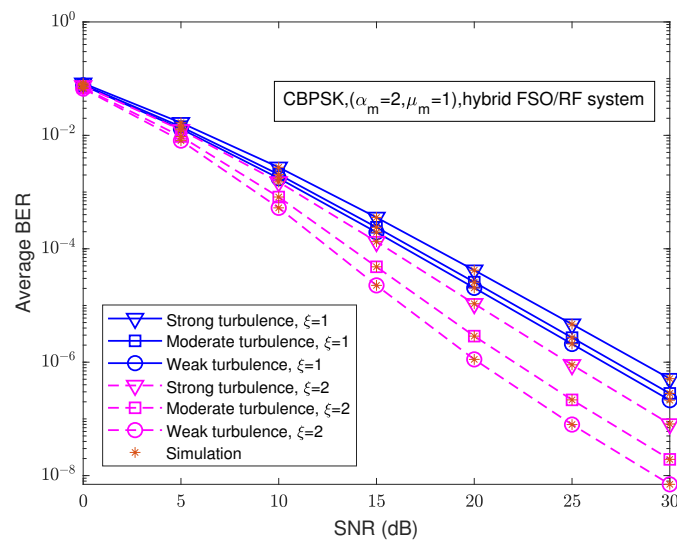


Figure 3. Relationship between BER and SNR of the hybrid system under different turbulence intensity and pointing errors.

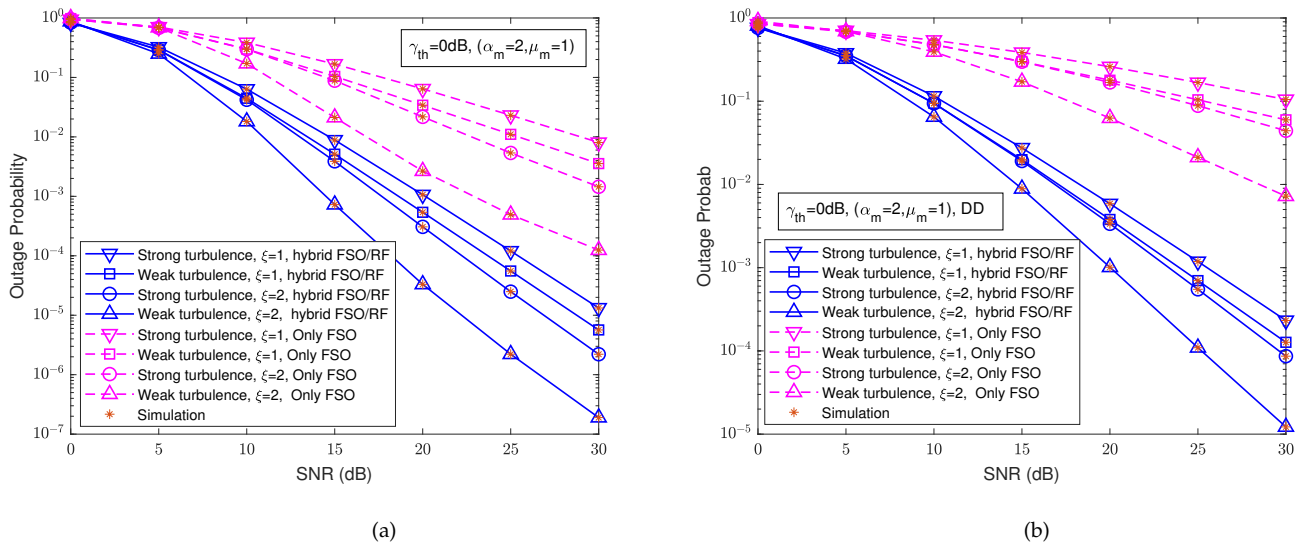


Figure 4. Relationship between OP and SNR of the hybrid system and only FSO system under different turbulence intensity, different pointing errors, and different detection techniques. (a) HD. (b) DD.

When the RF fading parameters are $(\alpha_m = 2, \mu_m = 1)$ and the decision threshold is $\gamma_{th} = 0$ dB, Figure 4 describes the relationship between the OP and the average SNR of the hybrid FSO/RF system and the only FSO communication system under different turbulence intensity, different pointing errors, and different detection techniques. Comparing Figure 4a,b, it is obviously found that the OP performance of the system with HD technique is better than that of DD technique whether it is an only FSO system or a hybrid system. As can be seen from Figure 4, compared with the only FSO system, the OP of the hybrid FSO/RF system is smaller, and the OP of the two systems decreases as the SNR increases. Assuming that the SNR is 20 dB, HD technique, $\xi = 2$, and the atmospheric turbulence intensity changes from weak to strong, the OP of the only FSO system are 2.66×10^{-3} and 2.173×10^{-2} , respectively, while the OP of hybrid system are 3.307×10^{-5} and 3.066×10^{-4} , respectively. From Figure 4, we can also find that the pointing errors have an impact on the OP performance of both the hybrid system and the single FSO system. Assuming that the SNR is 20 dB, HD technique, strong turbulence, and ξ changes from 1 to 2, the OP of the only FSO system are 6.418×10^{-2} and 2.173×10^{-2} , respectively, while the OP of hybrid system are 1.065×10^{-3} and 3.066×10^{-4} , respectively. Atmospheric turbulence, pointing errors, and detection techniques have a significant impact on the outage performance of both the only FSO system and the hybrid system, and the outage performance of the hybrid system is significantly better than that of the only FSO system.

When the FSO link environment is moderate turbulence, HD technique, RF fading parameters $(\alpha_m = 1, \mu_m = 1)$, and different pointing errors, Figure 5 shows the relationship between the ECC and the average SNR of the hybrid FSO/RF system with $\bar{\gamma}^{RF} = 10$ dB, the only FSO system, and the only RF system. Obviously, the atmospheric turbulence environment and pointing errors have no impact on the communication performance of the RF link, while the ECC of the hybrid FSO/RF system and only FSO system is affected by pointing errors. It can be seen from Figure 5 that the increase of ξ value means that the probability of beam alignment increases, resulting in the increase of channel capacity of the only FSO system and the hybrid FSO/RF system. It can be seen that when the FSO link is in a turbulent environment, the capacity of the hybrid FSO/RF system with MRC combination is much higher than that of the only FSO system and the only RF system.

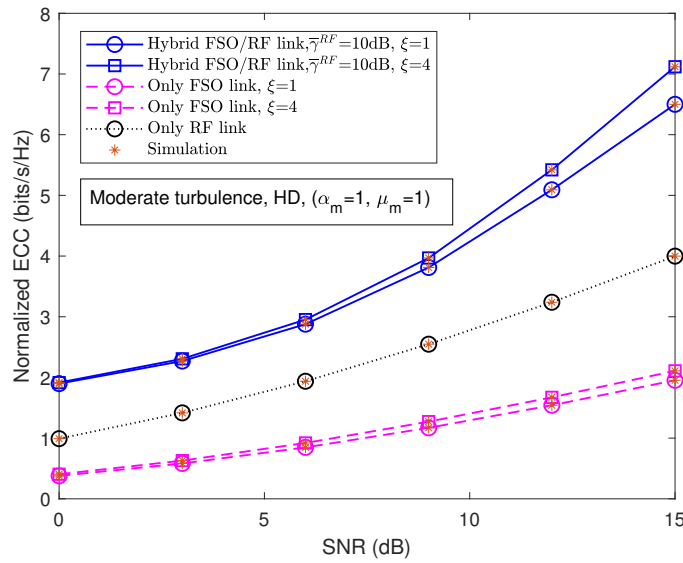


Figure 5. Relationship between channel capacity and SNR of the hybrid system, only FSO system and only RF system under different pointing errors and moderate turbulence.

Without losing generality, considering that the alignment of the FSO eavesdropping link is worse than that of the FSO communication link, assuming that the average SNR received by the eavesdropper is -5 dB and the target rate is 0.1 bit/s/Hz, ($\alpha_m = 2, \mu_m = 1$), $\bar{\gamma}^{RF} = 10$ dB, $\xi = 2$ and $\xi^E = 1$, Figure 5 shows that the relationship between the SOP of the hybrid system with FSO and RF link eavesdropping and the SNR of the FSO channel under different turbulence conditions. Figure 6 also shows that the SOP of the hybrid system will increase with the increase of turbulence intensity, whether FSO link eavesdropping or RF link eavesdropping. Therefore, it can be seen that whether FSO link eavesdropping or RF link eavesdropping, the turbulence intensity has an obvious impact on the SOP of the hybrid system. When the turbulence intensity is the same, the SOP of the system with RF link eavesdropping is higher than that with FSO link eavesdropping. It can be seen from Figure 5 that the capacity of the hybrid system is the highest, the only RF system is the second, and the only FSO system is the lowest. Therefore, the instantaneous security capacity of the hybrid system with RF eavesdropping is smaller than that with FSO eavesdropping. It is further known that the SOP of the hybrid system with RF eavesdropping is larger than that with FSO eavesdropping.

Assuming moderate turbulence and a target rate of 0.1 bit/s/Hz, ($\alpha_m = 2, \mu_m = 1$), $\bar{\gamma}^{RF} = 10$ dB, $\xi = 2$, and $\xi^E = 1$, Figure 7 describes the relationship between the SOP of the hybrid system with FSO link eavesdropping and RF link eavesdropping and the average SNR of the FSO channel under the different average SNR of eavesdroppers. When the average SNR of the eavesdropper increases, the SOP of the hybrid system increases accordingly. For example, when the average SNR of the FSO channel is 5 dB and $\bar{\gamma}^E = -5$ dB, the SOP of the hybrid system with RF link eavesdropping and FSO link eavesdropping is 1.87×10^{-3} and 5.927×10^{-4} , respectively; when average SNR of the FSO channel is 5 dB and $\bar{\gamma}^E = 0$ dB, the SOP of the hybrid system with RF link eavesdropping and FSO link eavesdropping is 2.16×10^{-2} and 7.809×10^{-3} , respectively.

Assuming moderate turbulence, ($\alpha_m = 2, \mu_m = 1$), $\bar{\gamma}^{RF} = 10$ dB, $\bar{\gamma}^E = 0$ dB, $\xi = 2$, and $\xi^E = 1$, Figure 8 describes the relationship between the SOP of the hybrid system with FSO link eavesdropping and RF link eavesdropping and the average SNR of the FSO channel under different target rates. The SOP of the hybrid system with RF eavesdropping link is higher than that of the FSO eavesdropping link. Whether FSO link eavesdropping or RF link eavesdropping, the SOP of the hybrid system further increases with the increase of the target rate. This is because when the target rate is increased, the SOP of the hybrid system also increases.

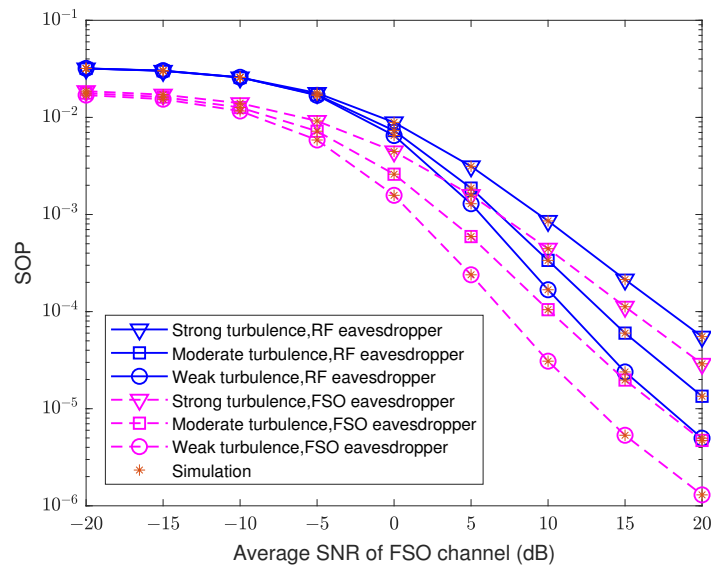


Figure 6. Under different turbulence intensity, the relationship between the SOP of the hybrid system with RF and FSO link eavesdropping and the average SNR of the FSO channel.

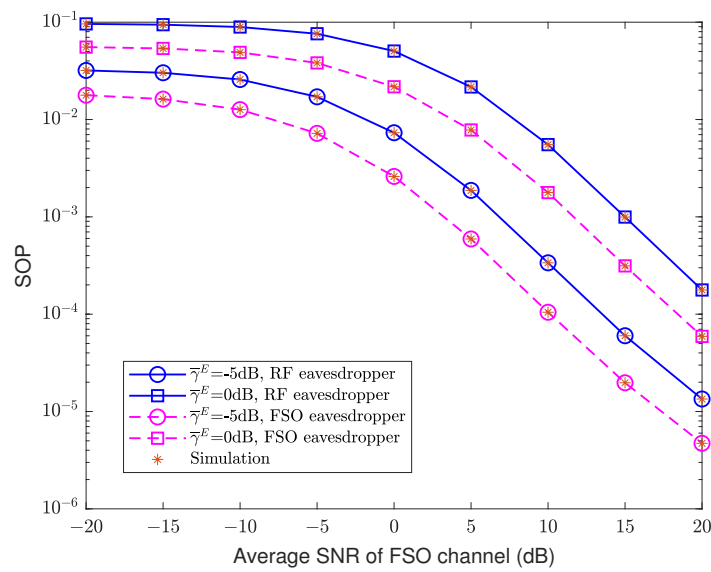


Figure 7. Under different $\bar{\gamma}^E$ conditions, the relationship between the SOP of the hybrid system with RF and FSO link eavesdropping and the average SNR of the FSO channel.

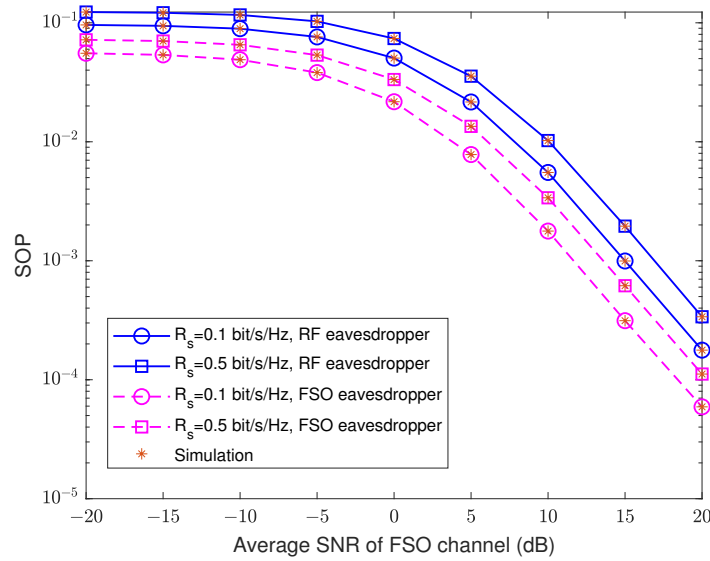


Figure 8. Under different R_s conditions, the relationship between the SOP of the hybrid system with RF and FSO link eavesdropping and the average SNR of the FSO channel.

Assuming moderate turbulence ($\alpha_m = 2, \mu_m = 1$), $\bar{\gamma}^{RF} = 10$ dB, $\bar{\gamma}^E = 0$ dB, and $R_s = 0.1$ bit/s/Hz, Figure 9 describes the relationship between the SOP of the hybrid system with FSO link eavesdropping and RF link eavesdropping and the average SNR of the FSO channel under different ζ and ζ^E . It can be seen from Figure 9 that whether it is FSO eavesdropping or RF eavesdropping, the SOP of the hybrid system decreases with the increase of ζ . According to Figure 5, as ζ increases, the capacity of the hybrid system also increases, so the SOP of the hybrid system with RF or FSO eavesdropping decreases. For example, when average SNR of the FSO channel is 12 dB and RF link eavesdropping, the SOP of the hybrid system with $\zeta = 3$ and $\zeta = 4$ is 2.6×10^{-3} and 2.55×10^{-3} , respectively; when average SNR of the FSO channel is 12 dB, $\zeta^E = 1$ and FSO link eavesdropping, the SOP of the hybrid system with $\zeta = 3$ and $\zeta = 4$ is 6.057×10^{-4} and 5.329×10^{-4} , respectively. It can also be seen from Figure 9 that the larger ζ^E , the larger the SOP of the hybrid system with FSO eavesdropping. For example, when the average SNR of the FSO channel is 12 dB, $\zeta = 4$ and FSO link eavesdropping, the SOP of the hybrid system with $\zeta^E = 1$ and $\zeta^E = 2$ is 5.329×10^{-4} and 21.146×10^{-3} , respectively.

Assuming that $\alpha_m = 2, \mu_m = 1, \bar{\gamma}^{RF} = 10$ dB, $\bar{\gamma}^E = 0$ dB, $\zeta = 2$, and $\zeta^E = 1$, Figure 10 describes the relationship between the SPSC of the hybrid system with FSO link eavesdropping and RF link eavesdropping and the average SNR of the FSO channel under different turbulence intensity. When the average SNR of the FSO channel is lower than 10 dB, the SPSC of the hybrid system with the RF link eavesdropping is lower than that of the FSO link eavesdropping; whether the RF link eavesdropping or the FSO link eavesdropping, the SPSC decreases with the increase of atmospheric turbulence intensity.

It can be noted that analytical results are perfectly matched with MC simulations presented in all figures.

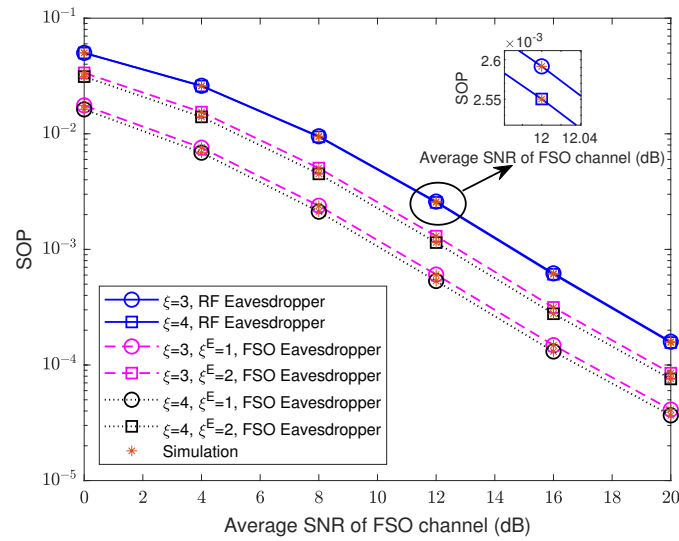


Figure 9. Under different ξ and ξ^E conditions, the relationship between the SOP of the hybrid system with RF and FSO link eavesdropping and the average SNR of the FSO channel.

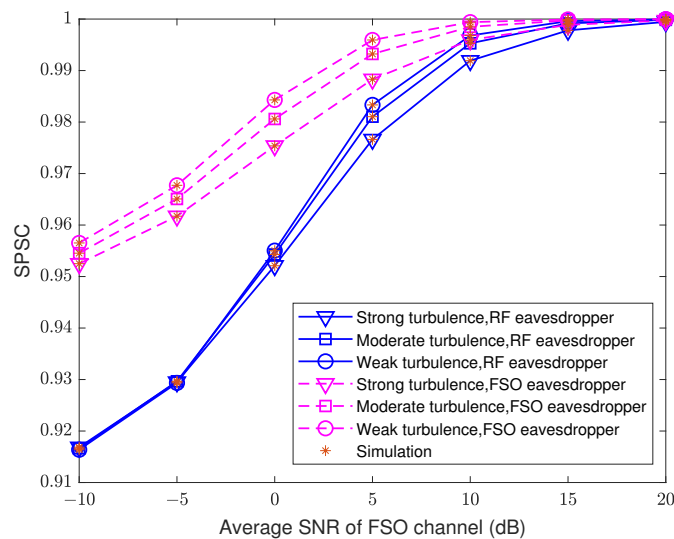


Figure 10. Under different turbulence conditions, the relationship between the SPSC of the hybrid system with RF and FSO link eavesdropping and the average SNR of the FSO channel.

6. Conclusions

This paper systematically analyzed the communication performance and security performance of the hybrid FSO/RF parallel transmission system with MRC technique, which was of great significance both in engineering practice and theoretical research. The channel model of the hybrid FSO/RF parallel transmission system over the Málaga turbulence and $\alpha - \mu$ fading was established, and then, the PDF and CDF of the output SNR of the hybrid system were obtained. Finally, the BER, OP, ECC, SOP, and SPSC of the hybrid system were analyzed, and their new-closed mathematical expressions were derived.

Through the simulation of the system, under the conditions of different modulation modes, different turbulence intensity, different RF fading parameters, and different pointing error parameters, the communication performance of the only FSO and the hybrid system, such as BER, OP, and ECC, were compared and analyzed; under the conditions of different turbulence intensity, different pointing error parameters, different target rates and different

average SNR of the eavesdropper, the SOP and SPSC of the hybrid system with the FSO link eavesdropping and the RF link eavesdropping were compared and analyzed. Among the three kinds of subcarrier modulation provided in this paper, the CBPSK modulation had the best BER performance of the only FSO and the hybrid system; with the increase of turbulence intensity, the communication performance and security performance of the hybrid system decreased; the ECC of the hybrid system with MRC technique increased with the increase of ζ ; as the beam jitter of the hybrid system decreased (i.e., the value of ζ increased), the BER, OP, SOP, and SPSC performance of the hybrid system improved, while the security performance of hybrid system with the FSO link eavesdropping decreased with the increase of ζ^E ; increasing the turbulence intensity, increasing the SNR of the eavesdropper, increasing the target transmission rate, and reducing the beam jitter of the FSO eavesdropper (i.e., the increase of ζ^E) could increase the SOP of the hybrid system, on the contrary, the SPSC of the hybrid system would be decreased.

Author Contributions: Conceptualization, Y.W. and D.K.; methodology, Y.W. and M.J.; software, Y.W. and G.L.; validation, Y.W. and M.J.; formal analysis, Y.W. and M.J.; writing—original draft preparation, Y.W. and D.K.; writing—review and editing, Y.W. and D.K.; supervision, D.K. All authors have read and agreed to the published version of the manuscript.

Funding: This research was funded by National Science Foundation of China (No. 62001333).

Institutional Review Board Statement: Not applicable.

Informed Consent Statement: Not applicable.

Data Availability Statement: Not applicable.

Conflicts of Interest: The authors declare no conflict of interest.

References

1. Abdalla, A.M.; Rodriguez, J.; Elfergani, I.; Teixeira, A. *Optical and Wireless Convergence for 5G Networks*; John Wiley & Sons: Hoboken, NJ, USA, 2019.
2. Magidi, S.; Jabeena, A. Free space optics, channel models and hybrid modulation schemes: A review. *Wirel. Pers. Commun.* **2021**, *119*, 2951–2974. [[CrossRef](#)]
3. Yasser, M.; Ghuniem, A.; Hassan, K.M.; Ismail, T. Impact of nonzero boresight and jitter pointing errors on the performance of M-ary ASK/FSO system over Málaga (\mathcal{M}) atmospheric turbulence. *Opt. Quantum Electron.* **2021**, *53*, 1–23. [[CrossRef](#)]
4. Li, M.; Cvijetic, M.; Takashima, Y.; Yu, Z. Evaluation of channel capacities of OAM-based FSO link with real-time wavefront correction by adaptive optics. *Opt. Express* **2014**, *22*, 31337–31346. [[CrossRef](#)] [[PubMed](#)]
5. Turan, H.; Subaşı, Ö. Development of Fine Tracking Unit for Hybrid ATP Mechanism in Free-space Optical Communication. In Proceedings of the 2021 29th Signal Processing and Communications Applications Conference (SIU), Istanbul, Turkey, 9–11 June 2021; pp. 1–4.
6. Wu, Y.; Mei, H.; Dai, C.; Zhao, F.; Wei, H. Design and analysis of performance of FSO communication system based on partially coherent beams. *Opt. Commun.* **2020**, *472*, 1–7. [[CrossRef](#)]
7. Li, K.; Lin, B.; Ma, J. Bit-error rate investigation of satellite-to-ground downlink optical communication employing spatial diversity and modulation techniques. *Opt. Commun.* **2019**, *442*, 123–131. [[CrossRef](#)]
8. Zhao, J.; Zhao, S.H.; Zhao, W.H.; Liu, Y.; Li, X. Performance of mixed RF/FSO systems in exponentiated Weibull distributed channels. *Opt. Commun.* **2017**, *405*, 244–252. [[CrossRef](#)]
9. Han, L.; Liu, X.; Wang, Y.; Li, B. Performance Analysis of Mixed Rayleigh and F Distribution RF-FSO Cooperative Systems with AF Relaying. *Electronics* **2022**, *11*, 2299. [[CrossRef](#)]
10. Kumar, K.; Borah, D.K. Quantize and encode relaying through FSO and hybrid FSO/RF links. *IEEE Trans. Veh. Technol.* **2014**, *64*, 2361–2374. [[CrossRef](#)]
11. Kumar, K.; Borah, D.K. Hybrid FSO/RF symbol mappings: Merging high speed FSO with low speed RF through BICM-ID. In Proceedings of the 2012 IEEE Global Communications Conference (GLOBECOM), Anaheim, CA, USA, 3–7 December 2012; pp. 2941–2946.
12. Vangala, S.; Pishro-Nik, H. Optimal hybrid RF-wireless optical communication for maximum efficiency and reliability. In Proceedings of the 2007 41st Annual Conference on Information Sciences and Systems, Baltimore, MD, USA, 14–16 March 2007; pp. 684–689.
13. Sharma, S.; Madhukumar, A.; Swaminathan, R. Switching-based cooperative decode-and-forward relaying for hybrid FSO/RF networks. *J. Opt. Commun. Netw.* **2019**, *11*, 267–281. [[CrossRef](#)]

14. Engelmann, A.; Jukan, A. Serial, parallel or hybrid: Towards a highly reliable transmission in RF/FSO network systems. In Proceedings of the 2015 IEEE International Conference on Communications (ICC), London, UK, 8–12 June 2015; pp. 6181–6186.
15. Shakir, W.M.R. Performance evaluation of a selection combining scheme for the hybrid FSO/RF system. *IEEE Photonics J.* **2017**, *10*, 1–10. [[CrossRef](#)]
16. Tahami, A.; Dargahi, A.; Abedi, K.; Chaman-Motlagh, A. A new relay based architecture in hybrid RF/FSO system. *Phys. Commun.* **2019**, *36*, 1–9. [[CrossRef](#)]
17. Altubaishi, E.S.; Alhamawi, K. Capacity analysis of hybrid AF multi-hop FSO/RF system under pointing errors and weather effects. *IEEE Photonics Technol. Lett.* **2019**, *31*, 1304–1307. [[CrossRef](#)]
18. Wu, Y.; Chen, J.; Guo, J.; Li, G.; Kong, D. Performance Analysis of a Multi-Hop Parallel Hybrid FSO/RF System over a Gamma—Gamma Turbulence Channel with Pointing Errors and a Nakagami-m Fading Channel. *Proc. Photonics* **2022**, *9*, 631. [[CrossRef](#)]
19. Yousif, B.B.; Elsayed, E.E.; Alzalabani, M.M. Atmospheric turbulence mitigation using spatial mode multiplexing and modified pulse position modulation in hybrid RF/FSO orbital-angular-momentum multiplexed based on MIMO wireless communications system. *Opt. Commun.* **2019**, *436*, 197–208. [[CrossRef](#)]
20. Elsayed, E.E.; Yousif, B.B. Performance enhancement of M-ary pulse-position modulation for a wavelength division multiplexing free-space optical systems impaired by interchannel crosstalk, pointing error, and ASE noise. *Opt. Commun.* **2020**, *475*, 126219. [[CrossRef](#)]
21. Sharma, S.; Madhukumar, A.; Swaminathan, R. MIMO Hybrid FSO/RF System Over Generalized Fading Channels. *IEEE Trans. Veh. Technol.* **2021**, *70*, 11565–11581. [[CrossRef](#)]
22. Usman, M.; Yang, H.C.; Alouini, M.S. Practical switching-based hybrid FSO/RF transmission and its performance analysis. *IEEE Photonics J.* **2014**, *6*, 1–13. [[CrossRef](#)]
23. Touati, A.; Abdaoui, A.; Touati, F.; Uysal, M.; Bouallegue, A. On the effects of combined atmospheric fading and misalignment on the hybrid FSO/RF transmission. *J. Opt. Commun. Netw.* **2016**, *8*, 715–725. [[CrossRef](#)]
24. Zhang, W.; Hranilovic, S.; Shi, C. Soft-switching hybrid FSO/RF links using short-length raptor codes: Design and implementation. *IEEE J. Sel. Areas Commun.* **2009**, *27*, 1698–1708. [[CrossRef](#)]
25. Vishwakarma, N.; Swaminathan, R. Performance analysis of hybrid FSO/RF communication over generalized fading models. *Opt. Commun.* **2021**, *487*, 126796. [[CrossRef](#)]
26. Shakir, W.M.R. On performance analysis of hybrid FSO/RF systems. *IET Commun.* **2019**, *13*, 1677–1684. [[CrossRef](#)]
27. Odeyemi, K.O.; Owolawi, P.A. Selection combining hybrid FSO/RF systems over generalized induced-fading channels. *Opt. Commun.* **2019**, *433*, 159–167. [[CrossRef](#)]
28. Vishwakarma, N.; Swaminathan, R. On the Capacity Performance of Hybrid FSO/RF System with Adaptive Combining Over Generalized Distributions. *IEEE Photonics J.* **2021**, *14*, 1–12. [[CrossRef](#)]
29. Liang, H.; Gao, C.; Li, Y.; Miao, M.; Li, X. Analysis of selection combining scheme for hybrid FSO/RF transmission considering misalignment. *Opt. Commun.* **2019**, *435*, 399–404. [[CrossRef](#)]
30. Chatzidiamentis, N.D.; Karagiannidis, G.K.; Kriezis, E.E.; Matthaiou, M. Diversity combining in hybrid RF/FSO systems with PSK modulation. In Proceedings of the 2011 IEEE International Conference on Communications (ICC), Kyoto, Japan, 5–9 June 2011; pp. 1–6.
31. Lei, H.; Dai, Z.; Ansari, I.S.; Park, K.H.; Pan, G.; Alouini, M.S. On secrecy performance of mixed RF-FSO systems. *IEEE Photonics J.* **2017**, *9*, 1–14. [[CrossRef](#)]
32. Lei, H.; Gao, C.; Guo, Y.; Pan, G. On physical layer security over generalized gamma fading channels. *IEEE Commun. Lett.* **2015**, *19*, 1257–1260. [[CrossRef](#)]
33. Juel, N.H.; Badrudduza, A.; Islam, S.R.; Islam, S.H.; Kundu, M.K.; Ansari, I.S.; Mowla, M.M.; Kwak, K.S. Secrecy performance analysis of mixed α - μ and exponentiated Weibull RF-FSO cooperative relaying system. *IEEE Access* **2021**, *9*, 72342–72356. [[CrossRef](#)]
34. Yang, L.; Liu, T.; Chen, J.; Alouini, M.S. Physical-Layer Security for Mixed η - μ and \mathcal{M} -Distribution Dual-Hop RF/FSO Systems. *IEEE Trans. Veh. Technol.* **2018**, *67*, 12427–12431. [[CrossRef](#)]
35. Mehta, H.; Sengar, S. Computation of Secrecy and Outages for Hybrid FSO/RF System with Modified Switching. In Proceedings of the 2021 IEEE 8th Uttar Pradesh Section International Conference on Electrical, Electronics and Computer Engineering (UPCON), Uttar Pradesh, India, 22 April 2021; pp. 1–6.
36. Shakir, W.M.R. Physical layer security performance analysis of hybrid FSO/RF communication system. *IEEE Access* **2020**, *9*, 18948–18961. [[CrossRef](#)]
37. Tokgoz, S.C.; Althunibat, S.; Miller, S.L.; Qaraqe, K.A. On the secrecy capacity of hybrid FSO-mmWave links with correlated wiretap channels. *Opt. Commun.* **2021**, *499*, 127252. [[CrossRef](#)]
38. Huang, L.; Liu, S.; Dai, P.; Li, M.; Chang, G.K.; Shi, Y.; Chen, X. Unified performance analysis of hybrid FSO/RF system with diversity combining. *J. Light. Technol.* **2020**, *38*, 6788–6800. [[CrossRef](#)]
39. Ansari, I.S.; Yilmaz, F.; Alouini, M.S. Performance analysis of free-space optical links over Málaga (\mathcal{M}) turbulence channels with pointing errors. *IEEE Trans. Wirel. Commun.* **2015**, *15*, 91–102. [[CrossRef](#)]
40. Jurado-Navas, A.; Garrido-Balsells, J.M.; Paris, J.F.; Puerta-Notario, A.; Awrejcewicz, J. A unifying statistical model for atmospheric optical scintillation. *Numer. Simulations Phys. Eng. Process.* **2011**, *181*, 181–205.

41. Yacoub, M.D. The α - μ Distribution: A Physical Fading Model for the Stacy Distribution. *IEEE Trans. Veh. Technol.* **2007**, *56*, 27–34. [[CrossRef](#)]
42. Zedini, E.; Soury, H.; Alouini, M.S. Dual-hop FSO transmission systems over Gamma–Gamma turbulence with pointing errors. *IEEE Trans. Wirel. Commun.* **2016**, *16*, 784–796. [[CrossRef](#)]
43. Ansari, I.S.; Al-Ahmadi, S.; Yilmaz, F.; Alouini, M.S.; Yanikomeroglu, H. A new formula for the BER of binary modulations with dual-branch selection over generalized-K composite fading channels. *IEEE Trans. Commun.* **2011**, *59*, 2654–2658. [[CrossRef](#)]
44. WolframsWebsite. Meijer-G. 2012. Available online: <http://functions.wolfram.com/PDF/MeijerG.pdf> (accessed on 1 August 2020).
45. Castillo-Vázquez, C.; Boluda-Ruiz, R.; Castillo-Vázquez, B.; García-Zambrana, A. Outage performance of DF relay-assisted FSO communications using time diversity. *IEEE Photonics Technol. Lett.* **2015**, *27*, 1149–1152.
46. Goldsmith, A.J.; Varaiya, P.P. Capacity of fading channels with channel side information. *IEEE Trans. Inf. Theory* **1997**, *43*, 1986–1992. [[CrossRef](#)]
47. Annamalai, A.; Palat, R.; Matyjas, J. Estimating ergodic capacity of cooperative analog relaying under different adaptive source transmission techniques. In Proceedings of the 2010 IEEE Sarnoff Symposium, Princeton, NY, USA, 12–14 April 2010; pp. 1–5.
48. Prudnikov, A. *Integrals and Series: Special Functions*; CRC Press: Boca Raton, FL, USA, 1986.
49. Springer, M.D. *The Algebra of Random Variables*; John Wiley & Sons: New York, NY, USA, 1979.
50. Anandani, P. Some integrals involving products of mieger’s G-function and H-function. In *Proceedings of the Indian Academy of Sciences-Section A*; Springer: Berlin/Heidelberg, Germany, 1968; Volume 67, pp. 312–321.
51. Singh, R.; Rawat, M.; Jaiswal, A. On the physical layer security of mixed FSO-RF SWIPT system with non-ideal power amplifier. *IEEE Photonics J.* **2021**, *13*, 1–17. [[CrossRef](#)]